Fabrication of Carbon-Aerogel Electrodes for Use in Phosphoric Acid Fuel Cells

By

Ronald S. Tharp

SUBMITTED TO THE DEPARTMENT OF MECHANICAL ENGINEERING IN PARTIAL FULLFILLMENT OF THE REQUIREMENTS FOR THE DEGREE OF

BACHELORS OF SCIENCE IN MECHANICAL ENGINEERING
AT THE
MASSACHUSETTS INSTITUTE OF TECHNOLOGY

JUNE 2005

Signature of Author: _____
Department of Mechanical Engineering
May 6, 2005

Certified by: _____
Ernest Cravalho
Professor of Mechanical Engineering
Thesis Supervisor

Accepted by: _____
Ernest Cravalho
Professor of Mechanical Engineering
Undergraduate Thesis Auditor

Fabrication of Carbon-Aerogel Electrodes for Use in Phosphoric Acid Fuel Cells

By

Ronald S. Tharp

Submitted to the Department of Mechanical Engineering
on May 6, 2005 in Partial Fulfillment of the
Requirements for the Degree of Bachelors of Science in
Mechanical Engineering

ABSTRACT

An experiment was done to determine the ability to fabricate carbon aerogel electrodes for use in a phosphoric acid fuel cell (PAFC). It was found that the use of a 25% solution of the surfactant Cetyltrimethylammonium chloride (CTAC) in water resulted in the creation of micelle within the pores of the organic aerogel. The micelle allowed the aerogel to be air dried while maintaining the desired pore composition. Further testing also showed that the resulting carbon aerogels had a specific ionic conductivity greater than that of a commercial porous carbon electrode

Work was done to explore the use of the DRIE method to create a silicone die for the fabrication of a carbon aerogel electrode. It was found that a die could be created but had to undergo O_2 plasma treatment in order to improve the wetting properties of the die. The resulting electrode was found to be very brittle at a thickness of 200 μm or less, but responded well to being electroplated with platinum through the use of a platinum salt and a non-ionic surfactant gel.

Thesis Supervisor: Ernest Cravalho

Title: Professor of Mechanical Engineering

Table of Contents

List of Figures

Chapter 1: Introduction

Ever since the energy crisis of the 1970's, research has been conducted to investigate alternative forms of energy that could replace fossil fuels. Currently no energy source has been found that can meet the demand levels and cost restraints necessary for an alternative energy source. As a result, some research has shifted to the realm of maximizing the efficiency of current energy sources. For example, many new power plants have converted from standard gas powered turbines to co-gen plants in which the excess heat from the power cycle is used for both heating and a secondary Sterling cycle. However, the heating aspect of a co-gen plant only remains viable within a small geographic radius.

A power alternative which has received significant attention and consideration is fuel cells. A typical fuel cell works by having an anode and cathode separated by an electrolyte. Hydrogen and oxygen gas are used in the reaction and the only waste product is water and heat. Fuel cells have been considered for use in cars. However, fuel cells have been found to be too expensive and heavy for this application. Hydrogen, a necessary fuel for fuel cells, need to be either stored within the vehicle or reformed from a higher energy density fuel stored in the vehicle. Both these options currently have technical and cost issues that make the eventual use of fuel cells in vehicles a long-term proposition.

A fuel cell becomes much more practical when its waste heat can be used. As such, an optimal scenario for the use of a fuel cell is for local power generation. A house or small group of houses could have a single fuel cell providing power. Excess heat could be used for heating during the winter and possibly cooling via an absorption refrigerator in the summer. In theory, a co-gen plant could provide similar services, but a co-gen plant is not as flexible to energy demands as fuel cells.

Therefore, a very promising role for fuel cells lies in medium-level energy production in the range of tens of kilowatts. The most commonly used fuel cell for this energy range is a phosphoric acid fuel cell or PAFC. PAFCs have been shown to be very reliable at this energy level and significant data exists for this type of fuel cell. Although PAFCs are well understood and reliable, they suffer the same problems as many other types of fuel cells: low ratios of energy to weight, volume, and price. As such their usage has not become very wide-spread.

The source of many of the inefficiencies of PAFCs lies at the cathode where oxygen gas reacts with hydrogen ions and electrons to produce water. The natural rate at which the reaction occurs is too slow, and as a result, platinum is used as a catalyst. However, the use of a catalyst creates a problem. In order for a reaction to occur, three components must be present: the oxygen in the form of a gas, the electrolyte in the form of a liquid, and the solid platinum catalyst. Therefore, the reaction demands that three separate phases be present at the same spot and at the same time for the reaction to occur at a practical rate.

Current methods used to fabricate cathodes are somewhat crude. Teflon is mixed with carbon black embedded with platinum to create an ink-like fluid. The ink is then sprayed onto a gas-permeable backing layer. The Teflon beads are non-wetting while the carbon agglomerates are wetting. As a result, thin films of electrolyte wets through the carbon agglomerates. Meanwhile, the Teflon beads create a path for oxygen to enter the ink layer. In the presence of a platinum particle, wherever films of electrolyte contacted an oxygen path, all three phases exist at the same time and the reaction can occur. The inherent problem with this method is that the arrangement of the carbon particles and Teflon are random. As such, much of the volume is wasted because agglomerates of carbon can exist where no film can reach it or where no path for the oxygen is present.

As such, our group sought to find ways to improve the performance of a phosphoric acid fuel cell by improving the cathode. The original thought process was that if an ink were used, the optimal arrangement of Teflon and carbon atoms would be achieved if all the carbon atoms were arranged in straight "finger-like" projections from the cathode with similar finger-like projections of Teflon beads projecting from the surface of the gas backing. As such, all carbon groups would be wetted by the electrolyte and every atom would be near a path for the oxygen gas.

This thought process eventually led to the idea of creating a porous substrate with a large porous volume and high permeability, into which larger pores would be microfabricated as shown in Figure 1.

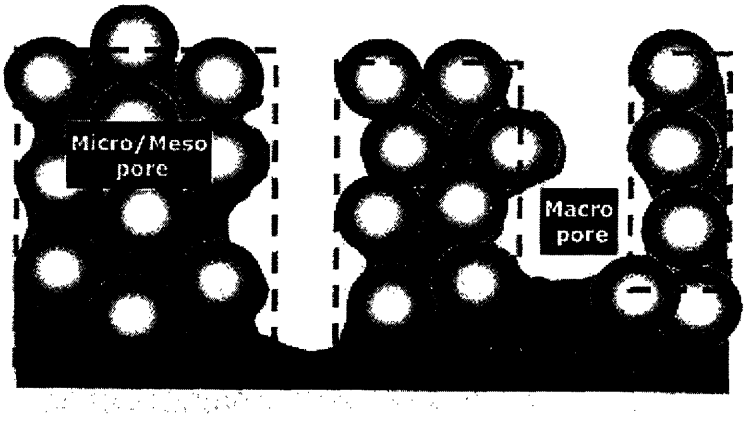

Figure 1: Depiction of Electrode Design Concept. The substrate is composed of micro and mesopores which are filled by electrolyte. Chemical reaction occurs on the surface of the large pores.

The porous substrate would act like the carbon black agglomerates and allow films of electrolyte to permeate the substrate. Due to the high permeability and pore sizes, the rate of ion transport within the substrate would be high. The large pores within the substrate would serve a similar function to the Teflon beads, allowing air/oxygen to enter the substrate. The advantage would be that an empty pore would eliminate the unnecessary volume of the Teflon beads and

allow optimal penetration of the oxygen into the substrate. A thin layer of platinum would be deposited on the surface of the larger pores. A positive pressure within the air entering the substrate would serve to counteract the capillary pressure of the electrolyte and keep the large pores evacuated. However, the larger capillary pressure of the smaller pores that make up the substrate keeps them saturated with the electrolyte and a thin film of electrolyte would exist on the surface of the platinum coating the channels. With this set-up, the solid platinum, liquid electrolyte, and gaseous oxygen would all be present. The thin nature of the electrolyte film would minimize the transport time of the oxygen to the platinum catalysts. Thus power production would be optimized.

In order to create the proper substrate, several factors were considered and tested. Carbon-aerogels were chosen to be the cathode substrate because of their high porosity, low density, high electrical conductivity, pore size, and high permeability. In order to create the large pores necessary for oxygen transport, a microscopic die was used. The die was created by using the Deep Reactive Ion Etching (DRIE) method. The last problem was finding the optimal way of drying the carbon-aerogel without suffering large volumetric shrinkage, cracking of the die, and the collapse of the pores within the aerogel itself.

Chapter 2: Previous Work and Concepts

2.1 Porosity

Any material that allows fluid flow through the material is classified as porous. A common way of describing a porous material is in terms of the size of the pores found within the material. Very small pores with diameter of less than 2 nm are referred to as micropores. In general, materials with micropores possess a large internal surface area. However, micropores are very resistant to fluid flow. This becomes a major issue, because many of the pores cannot be filled with fluid. If used as an electrode, the material would suffer from incomplete wetting and a slow replacement of fresh electrolyte.

An additional problem with micropores occurs when ions flow through the material. For a fuel cell, the working fluid is an electrolyte. In order for the reaction to occur, ions in the electrolyte outside of the cathode must travel into the cathode via the pores of the substrate. Usually, the rate of ion flow is dominated by molecular diffusion and migration. However, in the case of micropores, the diameter of the pores is small enough so that the walls of the pores hinder the rate of ion motion. Another way of describing this effect is that the ions "feel the presence" of the pore walls. Since ion flow is critical to the rate of energy production within a fuel cell, a material composed primary of micropores would be limited in terms of potential power production.

At the opposite end of the spectrum are large pores called macropores which have a diameter greater than 50 nm. Macropores do not limit ion flow and offer little resistance to fluid entry and flow. In addition, since macropores are so large, they are better able to resist collapse during the drying phase of organic aerogel fabrication. The problem with macropores is that they are, in effect, too large to be practical. During the operation of the fuel cell the electrode will contain oxygen at a pressure above that of the electrolyte. Some macropores can be large enough

to allow air to pass through the material and into the electrolyte, thus causing a "blow out." The release of oxygen into the electrolyte would taint the electrolyte and greatly decrease the power output of the fuel cell.

In between the previous types of pores are mesopores which have a pore diameter between 2 to 50 nm. Since mesopores are larger than micropores they are easily penetrated by fluids. More importantly, once saturated with an electrolyte, mesopores do not significantly influence ion motion through the electrolyte. Since mesopores are smaller than macropores, the risk of a "blow out" is minimized [1].

2.2 Carbon Aerogels

Carbon aerogels are most commonly created by the reaction between resorcinol (1, 3 dihydroxy benzene) and formaldehyde. The process is shown in Figure 2. The two components are mixed in a molar ratio of 2 formaldehyde molecules to 1 resorcinol in a solvent such as water or alcohol. Sodium carbonate is added to serve as a catalyst. The solution pH can be adjusted by the addition of dilute nitric acid. The presence of the catalyst results in the creation of ionized resorcinol by hydrogen abstraction from one of the OH group to form an O^+. The formaldehyde molecules then attach themselves to the carbon ring at either two of the 2, 4, or 6 sites to form a hydroxymethyl derivative of resorcinol containing two CH_2OH functional groups. The level of catalyst is important because it is the creation of the ionized resorcinol by the catalyst that dramatically increases the chances of formaldehyde bonding, which creates the resorcinol derivative that undergoes condensation [2].

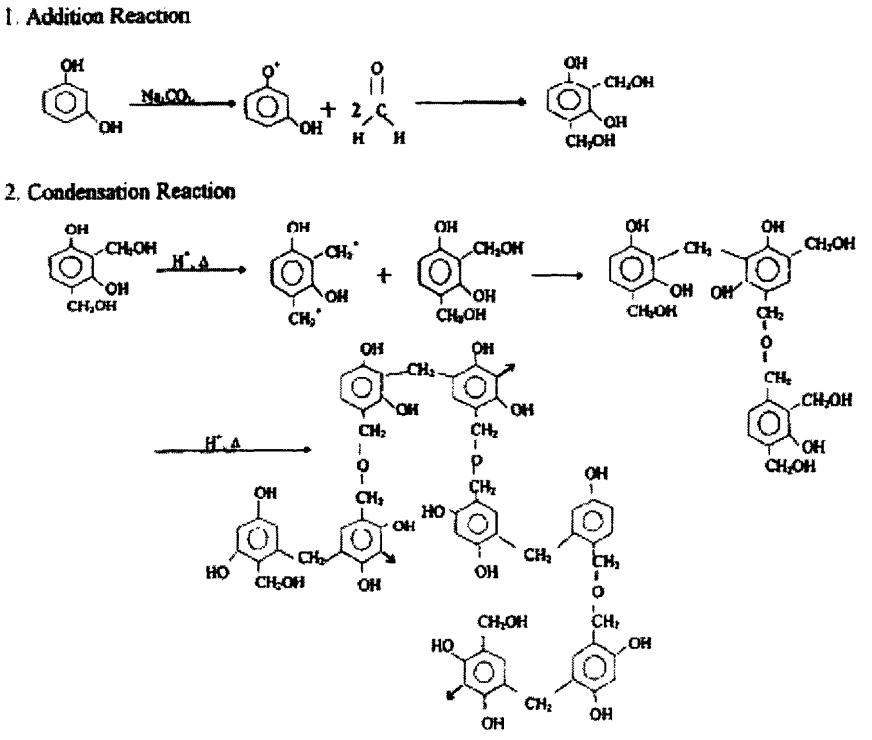

Figure 2: The Addition and Condensation Reactions Involved in the Forming of an Organic Aerogel [2]

During condensation, H^+ ions within the solution react to remove an OH^- group from one of the CH_2OH groups, thus creating a CH_2^+ group. The CH_2^+ from one resorcinol derivative usually joins itself to the benzene ring of another resorcinol derivative to create a methylene ($-CH_2-$) bridge. Sometimes the CH_2^+ may instead react with the CH_2OH group of another resorcinol derivative to create a methylene ether ($-CH_2OCH_2-$) bridge with an H+ ion as the byproduct [2]. Over time, the methylene ether bridges will disproportionate to form methylene bridges, forming formaldehyde as a byproduct. Depending on several factors, the curing time can vary from hours to days. During this time, monomers undergo further cross-linking to form nanometer-size clusters. Once a cluster is created, additional monomer groups attach themselves to the cluster. The result is that the cluster increases in size. The clusters continue to grow until all resorcinol is consumed. The size and appearance of the clusters within the gel structure vary heavily with the

ratio of resorcinol molecules to catalysts. With ratios between 50 and 300, a clear, red gel is formed. If the R/C ratio is set below 50, then the gel becomes opaque and contains precipitates [3].

After gelling is complete the gel has a complex structure of interconnected pores created by the intricate geometry of the joined particles. The next step is to evacuate the liquid solvent contained within the pores. The method used depends upon the solvent and several other elements of fabrication that will be discussed in a later section. In the most common case the solvent is water. Unfortunately, water has a very high surface tension of approximately 72.80 dynes/cm. Due to the low density of the aerogel and the small size of the pores, if the water were simply allowed to evaporate, its surface tension would render the aerogel useless by crushing all of the pores within the aerogel. In fact, almost any phase change process results in significant collapse of the pores.

The common solution is replacing the water with liquid CO_2. However, this is a long and complex process. Liquid CO_2 cannot directly replace the water. An organic solvent such as acetone must be used. The aerogel is soaked in acetone to allow the acetone to replace the water. Once the water has been replaced with acetone, the aerogel is placed within a high pressure chamber which is then filled with liquid carbon dioxide. Over the course of several days the liquid carbon-dioxide replaces the acetone within the pores. The temperature is slowly raised above the critical point of CO_2 at constant volume. Although the pressure is over 74 atmospheres, the degradation to the polymers is minimal. The super-critical carbon dioxide is vented until all carbon dioxide is removed. The pressure and temperature are returned to normal and the aerogel pores are left evacuated of liquid [3].

The organic aerogel is then pyrolyzed to create a carbon aerogel. During pyrolysis, the sample is placed within a nitrogen gas chamber. The temperature is then raised to between 800° and 1050° C. The bonds holding the hydrogen and oxygen atoms to the carbon skeleton break and

the hydrogen and oxygen are removed. Eventually, all that remains is the porous carbon skeleton of the aerogel, which is referred to as a carbon aerogel. Pyrolysis is accompanied with a decrease in volume of approximately 50%. The final density, surface area, and pore size depend upon variables in gel composition, gel drying, and pyrolysis.

2.3 Effect of R/C Ratio

The ratio of the amount of resorcinol to the amount of catalyst, also the called the R/C ratio, is an important element in determining the structure of the aerogel. The catalyst assists in the formation of the aerogel by ionizing the resorcinol molecules. The ionization of the resorcinol increases its propensity to react with formaldehyde to create functional monomer groups. The functional monomer groups cross-link to create nanometer-size clusters. Once a cluster is created, additional monomer groups will attach to the cluster. As the clusters grow in size, the surface area of the cluster and thus the number of reaction sites increase. The result is exponential growth in cluster size. Some of the methylene ether bridges break down to methylene bridges and release formaldehyde. Consequently, excess formaldehyde is always present and the particle growth continues until all the resorcinol is consumed [4].

The ratio of the resorcinol to the catalyst determines the likelihood of a cluster being formed. When the ratio has a small value, such as 50, the amount of catalyst is very large. The initial result is a significant number of clusters. With a large number of clusters each attracting resorcinol monomers, the rate of particle growth is slowed. The end effect is that more clusters exist and each cluster has a small diameter of between 3-5 nm. When joined, the particles have large necks, creating the fibrous appearance shown in Figure 3.

Figure 3: Image of Carbon Aerogel (RC = 50). Note the fibrous appearance. [4]

When the ratio is large, the amount of catalyst is fairly small. Fewer clusters are initially created, which results in less competition over resorcinol monomers. The clusters that do appear can easily grow in size. Due to how the number of reaction sites increases with volume, these clusters grow exponentially. The result is a small number of particles with large diameters between 11 and 14 nm. When joined, the particles have a "string of pearls"-like appearance as seen in Figure 4 [4].

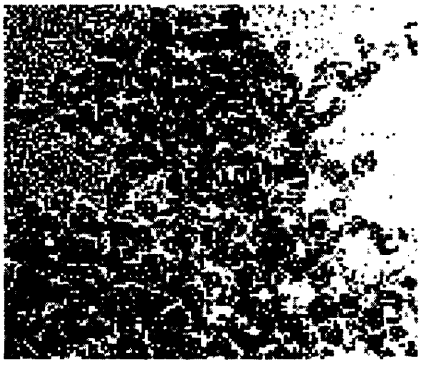

Figure 4: Image of Carbon Aerogel (R/C = 200). Note the "string of pearls" appearance and larger particle size [4]

In order to study the effect of RC ratio on particle size, V. Block et. al. [6] conducted research in which two different methods were utilized to find the average particle size of organic

aerogels and carbon aerogels with different R/C ratios. Small Angle X-Ray Scattering (SAXS) measurements were conducted on samples with RC ratios ranging from 100 to 1500, which was found to be the highest R/C ratio that allowed the sample to gel.

SAXS works by focusing a low divergence x-ray beam onto a sample. The x-rays are scattered by the particles within the material and create a pattern like the one shown in Figure 5.

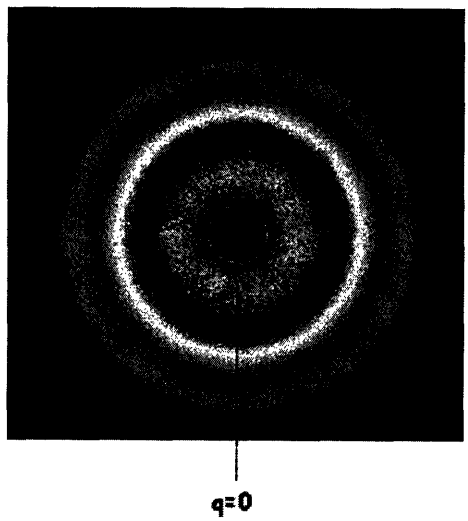

Figure 5: SAXS Image of a Carbon Aerogel. The center corresponds to a scattering angle of 0. [5]

An inverse relationship exists between the scattering angle and the feature size, so the scattering pattern image can be analyzed to determine the feature sizes within the aerogel. The results from the SAXS testing of organic aerogels are shown in Figure 6. In the figure, each plot line corresponds to a sample with a different R/C ratio. The lowest line corresponds to a sample with an R/C ratio of 100. The highest line is for a sample with an R/C ratio of 1500. For samples with an R/C ratio of 100 to 800, a clear cross-over exists. This crossover corresponds to the transition from "constant intensity toward zero scattering angle, into the asymptotic power law decay. [6]"

In general, the transition point shifts to lower scattering angles as the R/C ratio increases. Based upon the inverse relationship between feature size and scattering angle, a trend exists towards larger particle sizes as the R/C ratio increases. Thus, the model for aerogel formation is validated since high R/C ratios, corresponding to low levels of catalyst, result in larger particles.

After being pyrolyzed, nearly all samples undergo the same 50% reduction in size. In order to analyze particle size after pyrolysis, Block conducted SAXS testing on the carbon aerogel samples. The results are shown in Figure 7. As with the organic aerogels, the average particle size grows larger as the R/C ratio increases. Another important observation is that after pyrolysis the average particle size for a given R/C ratio increases. Although hard to see on the plot, the increase is indicated by the slight leftward shift of the transition point for samples with the same R/C ratio [6].

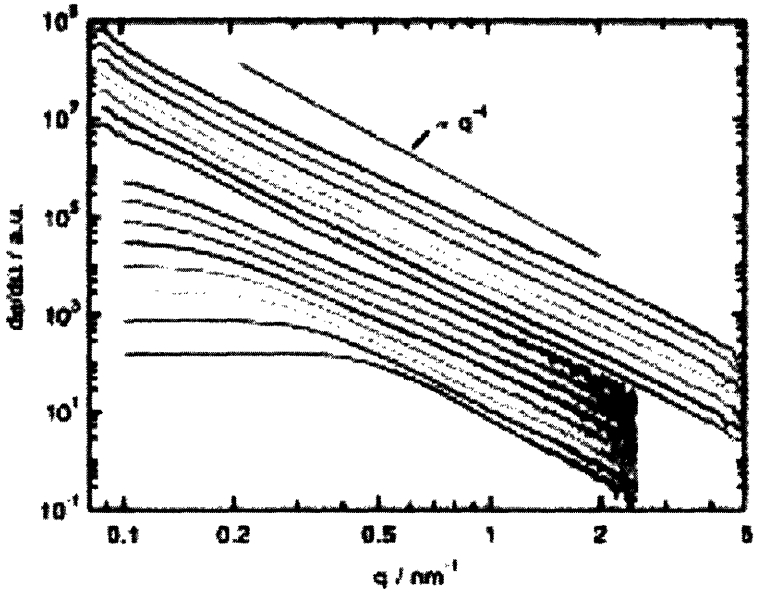

Figure 6: Data from SAXS Testing of Organic Aerogels Different R/C Ratios. Samples are vertically offset with the lowest line corresponding to an R/C ratio of 100, and the top line corresponding to an R/C ratio of 1500. The decrease in transition scattering angle corresponds to an increase in particle size [6]

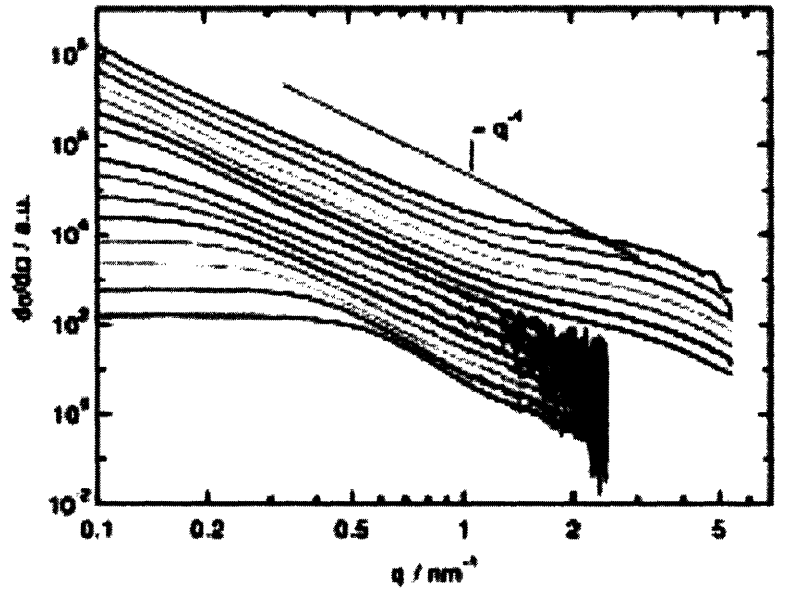

Figure 7: Data from SAXS Testing of Carbon Aerogels with Different R/C Ratios. The transition angle has decreased from Figure 5, representing an increase in particle size during pyrolysis [6]

The increase in particle size initially seems counter-intuitive. The particles have been stripped of all hydrogen and oxygen atoms and should have become smaller. The most likely reason for this increase in particle size is the joining of particles during pyrolysis. The high temperatures of the pyrolysis process result in partial graphitization of the particles which would lead to adjacent particles joining together.

Based upon the results of the SAXS testing, a theoretical model was developed in which the average particle size was related to the specific surface area of the aerogel. In order to provide a means of comparison, the BET (Brunauer, Emmett, and Teller) method for finding surface area and volume was also used. This method works by observing the amount of liquid nitrogen that is absorbed by the aerogel at different pressures. The levels of liquid nitrogen absorption can then be used to determine pore sizes, specific surface area, and volume [7]. The results from both types of testing for both the organic aerogel and the carbon aerogel are shown in Figures 8 and 9, respectively.

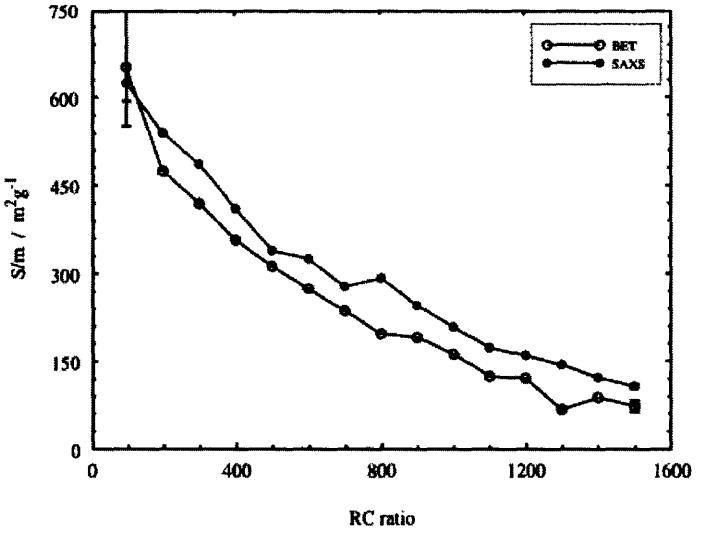

Figure 8: Surface Area vs. R/C Ratio for Organic Aerogels. Values were found by BET and SAXS methods. In general as R/C ratio increases, the surface area decreases [6]

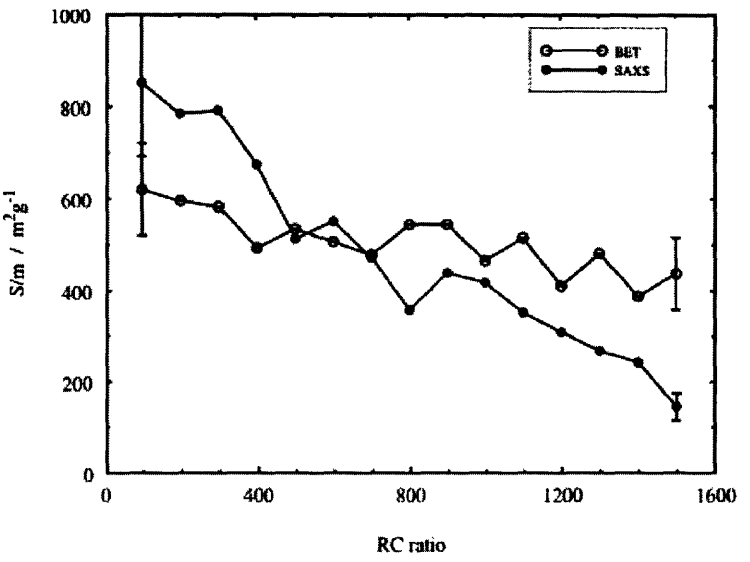

Figure 9: Surface Area vs. R/C Ratio for Carbon Aerogels. Values were found by BET and SAXS methods. In general as R/C ratio increases the surface area decreases. Ambiguities due to generation of micropores during pyrolysis [6]

Based upon these charts it appears that the specific surface area of both the organic aerogels and carbon aerogels increases as the R/C number decreases. However, the range of R/C ratios which would be used for an electrode lies between 50 and 300. Based upon the chart for the carbon aerogels, the decrease in specific surface area over this range is fairly small. In addition, a noticeable portion of the specific surface area for the lower R/C ratio aerogels is composed of micropores. As a result, the rate of ion transport, which is of more importance than surface area, would be limited.

2.4 Other Effects Influencing Carbon Aerogel Properties

In her 2002 paper, Emily Zanto [8] conducted experiments to determine how different factors would influence the final pore volume and surface area of a carbon aerogel. She also tested how the different factors influenced each other. An experimental method was used in which (k) factors were chosen. For her experiments, (k) was set as 3, with the factors being: the initial pH of

the solution, the initial solid-to-solution ratio, and the pyrolysis temperature used to create the carbon aerogel. For each of these factors (l) levels were set. For simplicity (l) was set to 2, corresponding to a high and low level for each of the (k) factors. The low level for pH was set at 5.5 and the high level was set as 7.0. The low value for weight percentage was set as 5% and the high level was set as 20%. The low value for pyrolysis temperature was set as 800° C, and the high temperature was set as 1050° C. In order to explore the relationship between these factors, 2^3 or 8 samples had to be produced and tested. The results of the testing are shown in Table 1 [8].

initial solution pH	solids content (wt %)	pyrolysis temperature (°C)	surface area (m^2/g)	pore volume (cm^3/g)	electrochemical capacitance (F/g)
5.5	5	800	561	0.32	128
5.5	5	1050	508	0.30	68
5.5	20	800	517	0.24	86
5.5	20	1050	474	0.23	59
7.0	5	800	900	0.92	179
7.0	5	1050	753	1.32	142
7.0	20	800	929	1.31	146
7.0	20	1050	804	1.42	144
		average =	680.8	0.758	119.0
		standard deviation =	186.6	0.539	42.9

Table 1: Material Properties from Testing of Fabrication Variables. Every variable has a high and low value and each value is used 4 times [8]

After testing, each variable was analyzed using Taguchi's statistical design method. Based upon that analysis, two plots were created and are reproduced below. The first plot is a Pareto plot which shows the relative magnitude of the effect of each of the 7 variable combinations. The dashed line indicates the 90% confidence limit. Any variable which exceeds that threshold can, within a 90% level of certainty, be said to have a significant effect on surface area. As can be seen the only variable which exceeds that threshold is initial pH. However, pyrolysis temperature

almost exceeds that threshold and thus should also be considered an important variable. Also of note is the fact that weight percentage has almost no effect on surface area [8].

Figure 10b provides similar evidence of the relative effect of each variable. Q indicates the standardized effect of each variable. Zanto: "The z-score is an indicator of the cumulative probability of the normal distribution [8]." Ideally, any insignificant variable would lie on a vertical line with a Q-value of 0. This would indicate the variable had no effect. However, theoretically, all points which tend to create a line with a small slope which goes through the (0, 0) point of the plot can also be considered to correspond to a factor or combination of factors that have no effect. On the plot, the points corresponding to all factors other than pH and pyrolysis temperature create a clear straight line through the (0, 0) point of the plot. Thus, all factors and combinations corresponding to those points have statistically no effect. The point corresponding to initial pH is very distant from the line corresponding to zero effect and has a very high Q-value. The point corresponding to pyrolysis temperature does not lie on the line of zero effect but is not very distant from the line. Therefore, supporting what is shown in (10a), the pH has a significant effect and pyrolysis temperature has somewhat of an effect on surface area.

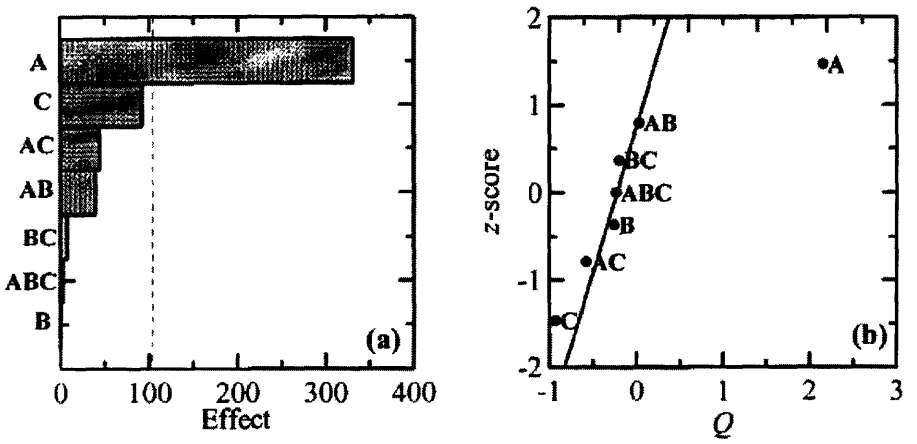

Figure 10: (a) Pareto Plot and (b) Normal Probability Plot for the effects of (A) initial pH, (B) weight percentage of solids, and (C) pyrolysis temperature, on the surface area of carbon aerogels. Dashed line in (a) corresponds to a confidence limit of 90% [8]

2.5 Effect of pH

The complex chemical reaction which results in the formation of an RF gel appears to be one that is highly dependent on the pH of the solution. The most likely reason for this dependence is the chemistry of the two reactions which dominates the formation of the organic aerogel. The first reaction is the ionizing of the resorcinol molecule to promote the reaction between the resorcinol and formaldehyde. This reaction requires sodium carbonate as a catalyst to aid in the removal of an H^+ ion from the one of the hydroxyl groups on the resorcinol molecule. Solutions with low acidity make removal of hydrogen ions easier. In addition, the solutions must not be too acidic or the sodium carbonate will be consumed. The other critical reaction is the cross-linking that occurs as a result of the removal of an OH^- group from the hydroxyl-methyl groups of the resorcinol derivates. This reaction requires that H^+ ions be present and thus is promoted by the solution being acidic.

Since the chemical reactions which create the aerogel require that the solution be neither too acidic nor too basic, it seems logical that the optimal pH for the solution would be neutral or

only mildly acidic. As such, the basic salt would not be consumed and could activate the resorcinol molecules. Meanwhile, enough H^+ ions would be present to remove an OH^- from one of the CH_2OH groups to allow for cross-linking. The results of pH testing, shown in Figures 11 and 12, demonstrate this assumption to be correct, since surface area and volume both increase as solutions become more neutral.

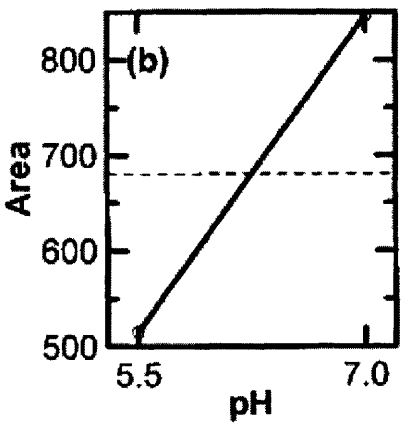

Figure 11: Effect of pH on Surface Area for Carbon Aerogels. The surface area increases and the pH increases [8]

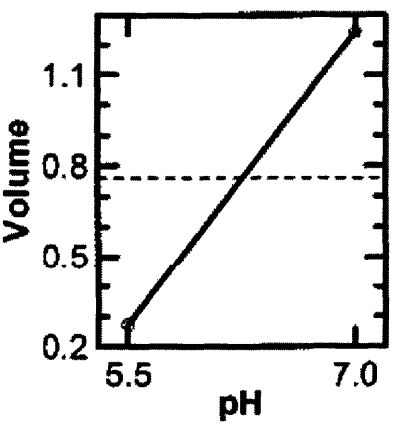

Figure 12: Effect of pH on Volume for Carbon Aerogels. As with surface area, volume increases as surface area increases [8]

2.6 Effect of Pyrolysis Temperature

As shown in Figure 13, pyrolysis appears to have a negative effect on the surface area of the carbon aerogel. During the pyrolysis process, the organic aerogel is heated to remove all oxygen and hydrogen atoms from the carbon skeleton. In order to do so, the temperature must be high. However, at higher pyrolysis temperatures, some of the carbon particles will undergo a chemical reaction in which they shift from simple carbon particles to graphite. In regions where this happens, the graphite particles will tend to attach themselves to adjacent graphite and carbon particles. The net effect is a reduction in the number of particles and a decrease in the overall surface area.

Thus, if surface area and pore composition were the only concern, then the lower pyrolysis temperature would be optimal. However, the removal of all organic compounds and non-carbon molecules from within the aerogel is critical. If these atoms and compounds remain after pyrolysis, then they will interfere with the chemical reactions within the fuel cell. In addition, the presence of these unwanted compounds and atoms also provides an x-factor in all performance analyses. Therefore, when considering the optimal pyrolysis temperature, the decision should not be made solely on the resulting surface area, especially since the use of the high pyrolysis temperature only seems to reduce surface area by 10 %.

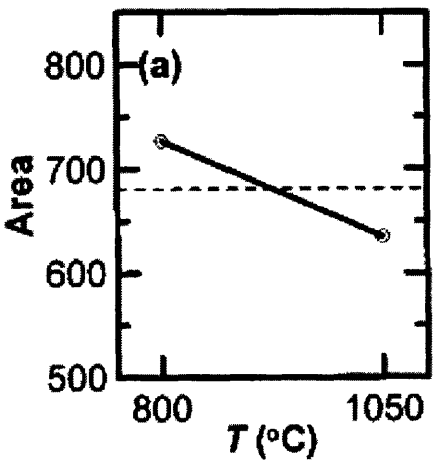

Figure 13: Effect of Pyrolysis Temperature on Surface Area of Carbon Aerogels. Surface area decreases as temperature increases, likely due to particle joining [8]

2.7 Surfactants in Aerogel Fabrication

The greatest contribution to the collapse of pore structures is the surface tension of the solvent, which is present inside the mesopores of the aerogel. The most common solvent has been water. However, due to water's high surface tension, other solvents and solvent exchange methods have also been explored. Since the most complicated, time consuming, and expensive step in carbon aerogel fabrication is the supercritical CO_2 drying, work has been done to see if that step could be removed. A revolutionary idea was to use surfactants within the solvent.

Surfactants are compounds which have both a hydrophobic and hydrophilic end. The hydrophilic end tends to orient itself towards polar molecules when it is in a solution. The hydrophobic end tries to orient itself toward non-polar molecules and away from polar molecules as much as possible.

In a recent patent application, Bell et. al explored the possibility of using a water and surfactant solution during organic aerogel fabrication to remove the need for supercritical CO_2 drying. The key to the use of surfactants is that water is very polar. The surfactant in the

resorcinol-formaldehyde solution aligned themselves with their hydrophobic heads facing the solution and their hydrophobic tails facing each other. The resorcinol-formaldehyde polymer forms around these surfactant micelles as seen in Figure 14 [1]. The size of the micelles is related to the initial concentration of surfactant in solution. Generally, a solution with higher surfactant concentration will have larger micelles and result in aerogels with larger pores. Bell [1] found by adjusting the initial formulation of the solution, carbon aerogels can be formed with a narrow pore size distribution and with average pore sizes in the rage of 4nm to microns.

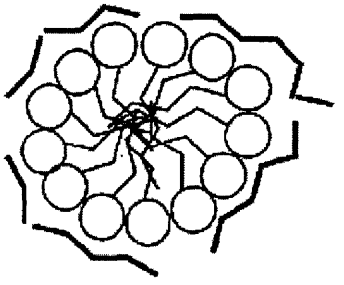

Figure 14: Depiction of the Micelle Created by the Surfactant within the Pore. The micelle braces the pore and reduces the effect of the water surface tension [1]

The creation of the micelle has three primary advantages. The first advantage is that the usual diameter of the liquid crystal is such that it encourages the creation of mesopores rather than micropores. Since mesopores have the optimal properties for a fuel cell electrode, the presence of the micelle should improve the performance of the electrodes manufactured using this method. The second advantage is that the contact between the water and the pore walls is reduced, thus decreasing the effective surface tension of the water. As a result, during the process of drying, the amount of stress placed on the walls is lower than if the surfactant were not used. The third advantage is that the micelle remains during the drying process. As such, the crystal acts like a series of struts bracing the pore walls against each other.

The combination of these three effects greatly reduces the likelihood of collapse. In fact, the effect is so significant that aerogels can be dried without having to replace the water solvent; while still possessing a structure comparable to aerogels created by super-critical CO_2 drying. After air drying, the micelle are consumed by the pyrolysis process, leaving little trace. Thus, the use of surfactants allows for air drying without solvent exchange, while preserving the geometry of the aerogel and leaving no residue [8].

2.8 Deep Reactive Ion Etching (DRIE)

DRIE was used to fabricate the silicone die which was used as the negative template for the electrode design. An example of a DRIE machine (Surface Technology Systems, Newport, Gwent, UK) is shown in Figure 15 (9)

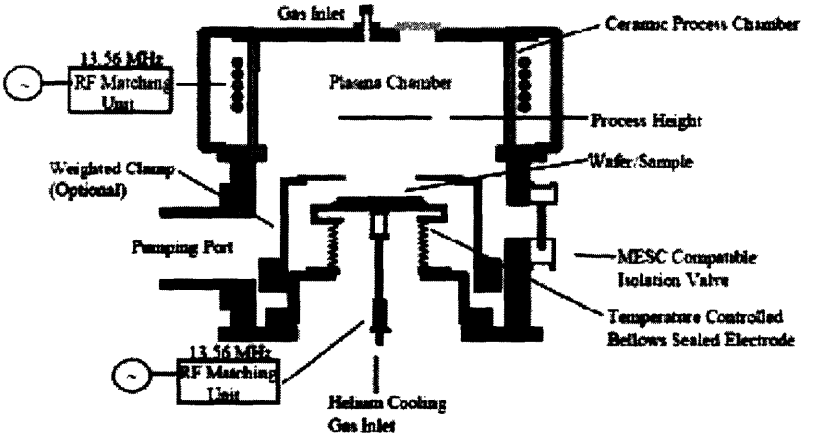

Figure 15: Example of Apparatus used for DRIE [9]

The main chamber is composed of an inert porcelain reaction chamber into which the sample is placed. The reaction chamber is surrounded by a radio frequency (RF) coil which is powered by 1000 W power supply operating with a frequency of 13.56 MHz. An additional power supply, also

operating at 13.56 MHz is connected to the wafer itself in order to "vary the RF bias potential of the wafer with respect to the plasma. This arrangement permits the independent control of the energy of the ions reaching the substrate as well as the ion flux. [10]"

A turbopump is used to maintain a low pressure within the reaction chamber. The etching gas, usually SF_6, enters the chamber through its top. Radio frequency coils on either side of the main chamber excite the gas into a plasma state [10].

The plasma interacts with the exposed surfaces of the silicon wafer, etching the surface. The chemical byproducts are removed from the chamber to prevent them from becoming redeposited. Due to the high energy nature of the system and the plasma gas, the wafer temperature is maintained through the use of a helium gas cooling system placed on the backside of the wafer [9].

The simplified chemical reaction that creates the plasma is shown in Eq. 1

$$SF_6 + e^- \longrightarrow S_xF_y + S_xF_y^{\bullet} + F^{\bullet} + e^- \qquad \text{Eq. 1}$$

in which the etching gas SF_6 is excited and creates ions S_xF_y and plasma $F^{\bullet}$. When the $F^{\bullet}$ plasma comes in contact with the silicone atoms, a chemical reaction occurs. The reaction is described in Equation 2.

| Eq. 2

The reaction byproducts are then removed, thus etching the surface [9].

In normal reactive ion etching (RIE), the allowable aspect ratio of depth to height and wall straightness is limited by the fact that the process of etching the hole also etches away the sidewalls of the hole. As such, the channel develops an isotropic profile without straight walls. In order to solve this problem, the flow of etching gas is cyclically stopped. The gas, C_4F_8, is then injected into the chamber. The gas coats the surface of the silicon, including the walls and the bottom of the etchings [11]. This coating is chemically resistant to the fluorine plasma and thus acts as a

passivating gas to the etching reaction. However, the bottom of the hole is bombarded by S_xF_y ions which quickly erode the coating. The coatings on the walls are less affected due to their indirect exposure to the ionic bombardment [11]. The process is shown in Figure 16.

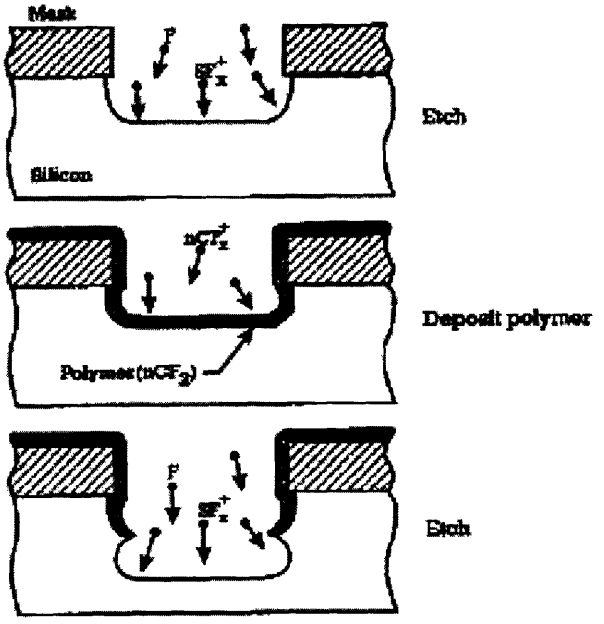

Figure 16: Depiction of the Etching and Polymer Deposit Process of DRIE. Notice that the side wells are less exposed to ionic bombardment and that the walls develop a scalloped appearance [11]

The process of alternating flows of etching gas and passivating gas is shown in Figure 17. The overlap is due to the non-instantaneous response of the flow controllers. Each etching sequence increases the depth of the hole [10]. Build-up of the passivating coating is minimized since ion exposure increases as a function of distance from the wall.

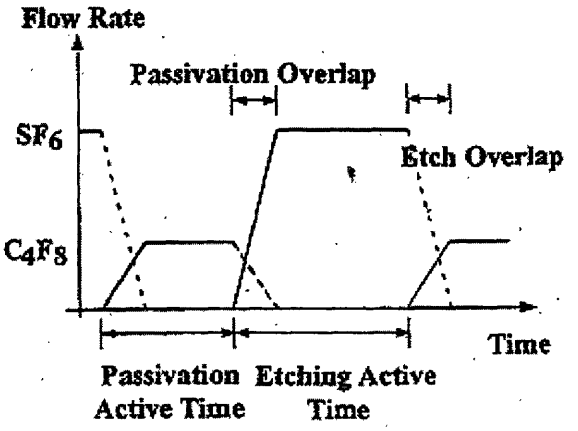

Figure 17: Alternating Sequence of Etching Gas and Passivating Gas used in DRIE [10]

One side effect of this method is that since each cycle of etching does in fact produce a slightly isotropic wall, the sides of the wall appear scalloped when observed closely enough, as shown in Figure 18. However, the effect can be minimized by shortening the length of the etching cycle. The only drawback is the large increase in etching time [10].

Figure 18: Image Showing the Scalloping Generated by DRIE [10]

Chapter 3: Ionic Conductivity Testing of Carbon Aerogels

An important property for any electrode is its ionic conductivity, which measures how easily a current can pass through the electrolyte contained within. Sample electrodes made with and without surfactants were produced and tested along with a commercially-produced porous carbon electrode. All samples were cut to be 1 cm in diameter.

3.1 Experimental Set-Up

The experimental set-up is shown in Figure 19. An inert and electrically non-conductive chamber was filled with 85% phosphoric acid. Phosphoric acid was used because of its well-known properties and because phosphoric acid will be used as the electrolyte in the final fuel cell design. Two electrodes were introduced into the phosphoric acid bath at either end of the chamber. Two reference electrodes were also introduced into the phosphoric acid bath between the two electrodes. Guide holes at the top of the chamber kept the distances between all components of the apparatus constant.

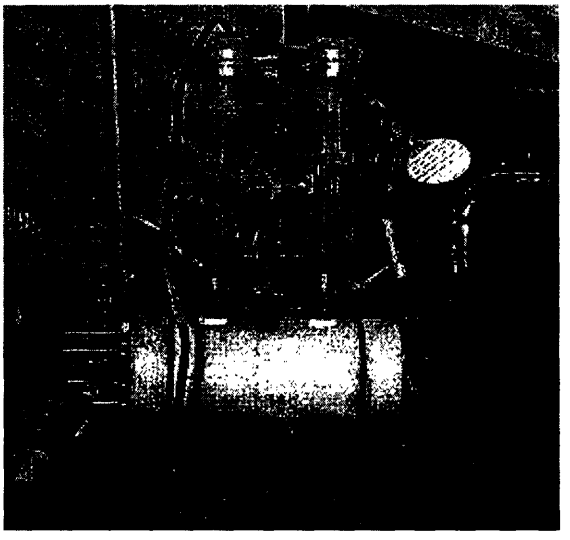

Figure 19: Picture of Apparatus used for Ionic Conductivity Testing

3.2 Procedures

A current source was connected to the two electrodes. A set current was then passed through the electrodes and the phosphoric acid bath without an aerogel between the Pt electrodes. The reference electrodes measured the voltage potential. The voltage of the apparatus was measured at ten different current levels.

The porous aerogels were then soaked in a similar 85% phosphoric acid solution for one day. This was done to ensure that the pores of the aerogel were completely saturated with phosphoric acid. The aerogels were then placed between the two reference electrodes. The same set of currents that were passed through the apparatus without the sample is used with the samples in place. The resulting voltage potentials were once again measured by the two reference electrodes. The schematic for the system is shown in Figure 20.

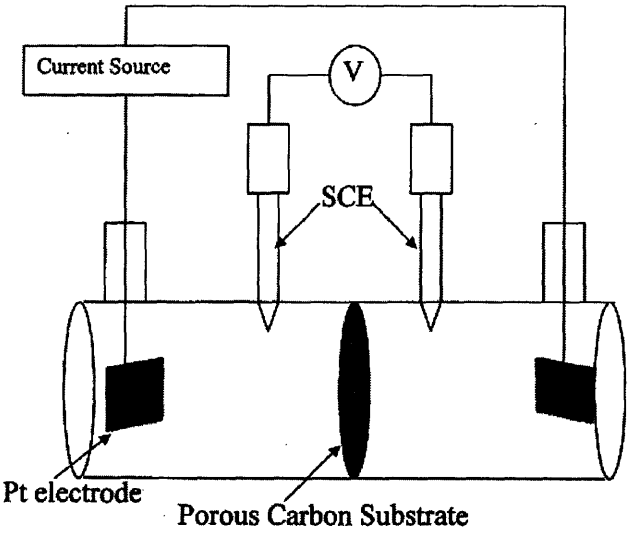

Figure 20: Schematic of Ionic Conductivity Testing Apparatus

The measured voltage potentials were plotted in terms of the currents. Best-fit lines were found for the voltages with and without the samples in place. The resulting plots and best-fit lines for the sample with a CTAC/R ratio of .06 are shown in Figure 21.

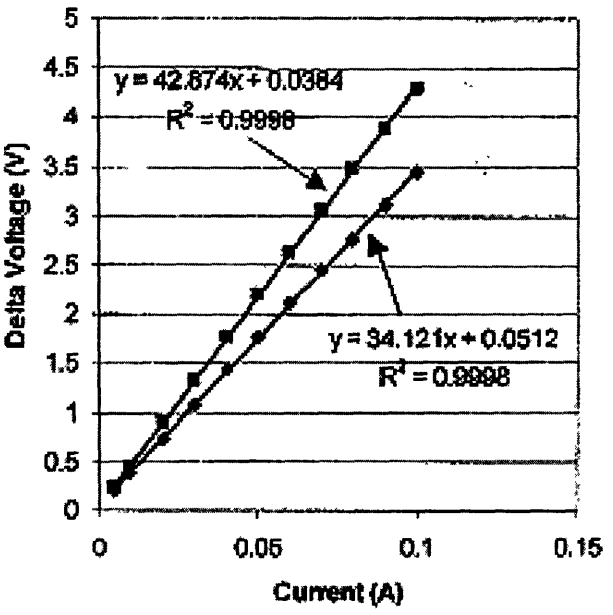

Figure 21: Voltage Drop vs. Current for Apparatus. The bottom line is the resistance when no sample is in place. The top line is an example from when a sample with a CTAC/R ratio of .06 was in place. The slope of the line indicates the resistance

The data demonstrated linear behavior and a high level of agreement with the best-fit line, as shown by an R value of .9998. According to Ohm's law, resistance can be found by using Equation 3

$$R_{\Omega} = V/I \qquad \text{Eq. 3}$$

in which R_{Ω} is resistance, V is measured voltage, and I is current. Thus, the resistances of the system with and without the samples were found as the slope of the best fit line from the voltage vs. current plots. The resistance of the system without a sample (R_{base}) was found to be 34.121 Ohms. The resistance of the system when a sample was present (R_{sample}) was found using the same method. The ionic conductivity of a sample was then found using Equation 4.

$$\sigma_{effective} = \frac{l}{(R_{with\ sub} - R_{base})S} \qquad \text{Eq. 4}$$

where l is the thickness of the aerogel and S is its area exposed to the electric field.

Four different aerogel types were tested using this method. The preparation procedure for each of these aerogels is given below.

Organic aerogels via air drying with a low surface tension fluid

In this case two aerogel were made with different R/C ratios. One aerogel contained an R/C ratio of 50 which represented the highest level of catalyst that could be added without precipitate formation. The other had an R/C ratio of 200, which corresponds to a low level of catalyst. Water was used as the solvent in the resorcinol-formaldehyde solutions. Each solution was sealed in an airtight vial and cured by spending 24 hours at room temperature, then 24 hours at 50°C, and finally an additional 24 hours at 90°C. Next, the water was exchanged with acetone and then with cyclohexane. The two samples were then allowed to air dry at room temperature to remove the cyclohexane.

Organic aerogels air dried with the aid of a surfactant

Two aerogel samples were made using the surfactant method described by Bell [1]. Both samples were formed with an R/C ratio of 200. In one sample, the molar ratio of surfactant cetyltrimethylammonium (CTAC) to resorcinol was 0.06. For the other sample, the ratio was set at 0.1. These samples were then cured for 24 hours at 70° Celsius. Finally, the samples were air dried for 24 hours at room temperature followed by three hours within a 100° C convection oven.

All four samples were placed within an inert N_2 atmosphere oven. The temperature was increased by $1^\circ C/\text{min}$ until the temperature reached 1050° C. The samples were then kept at this temperature for 4 hours, during which the sample underwent pyrolysis, leaving a carbon skeleton.

The structure of the samples was explored by using a Scanning Electron Microscope to take pictures of the surface of each sample type. The density and average poor size of the samples was also measured.

3.3 Experimental Results

The density, average pore size, and other elements are summarized in Table 2. The SEM images of the surfaces of each sample can be seen in Figure 22.

No Surfactant

R/C	Density (g/cm^3)	Avg. Pore Size (nm)	Porosity
50	1.2	N/A	0.155
200	1.0	< 30	0.30

Surfactant (R/C = 200)

CTAC/R	Density (g/cm^3)	Avg. Pore Size (nm)	Porosity
0.06	0.65	100	0.54
0.10	0.55	500	0.61

Table 2: Material Properties for Carbon Aerogel Samples for different R/C ratios and CTAC/R ratios. The surfactant samples have a lower density, continuous porosity, and larger mesopores

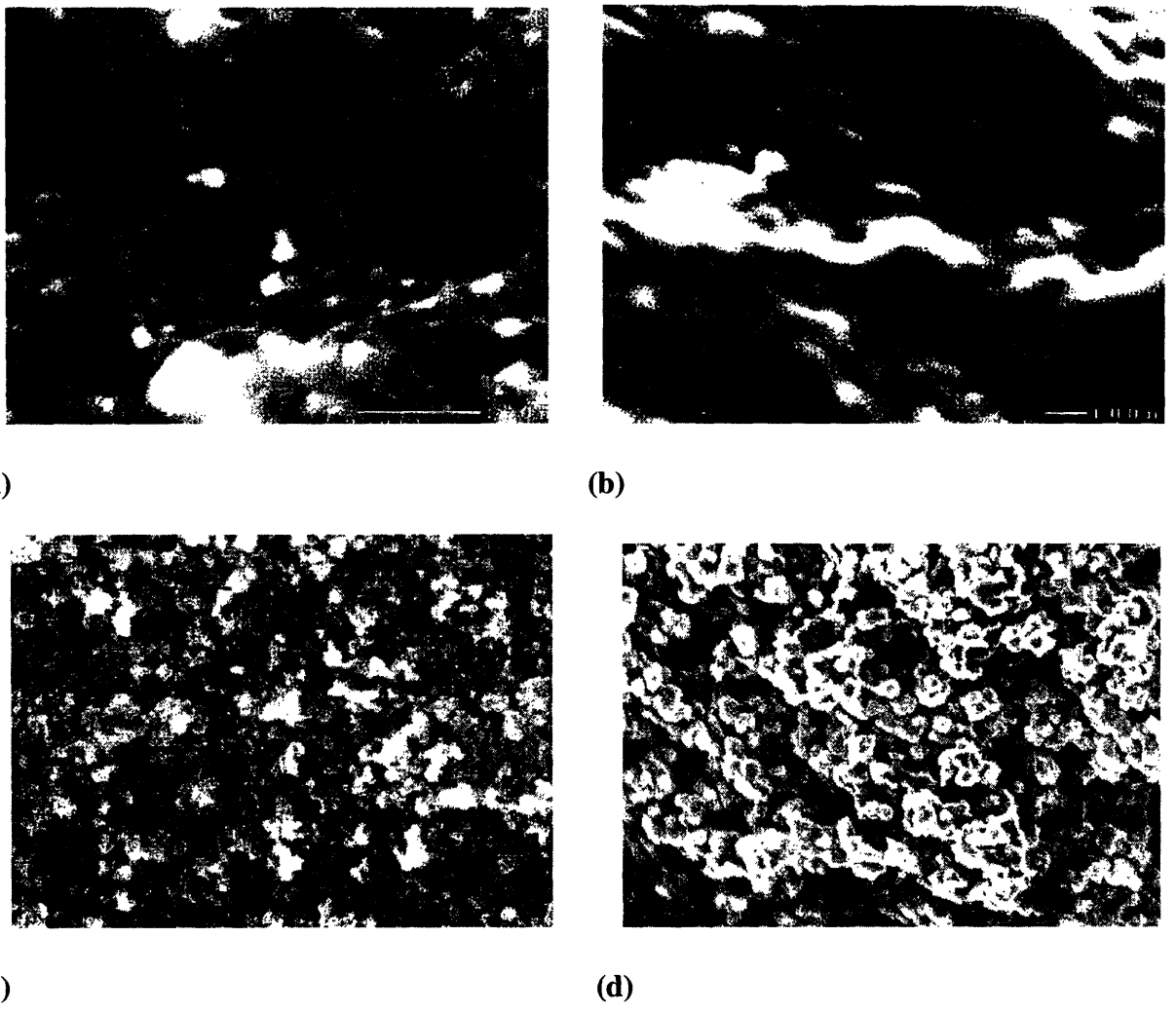

Figure 22: SEM images of Surfaces of Carbon Aerogels. (a) R/C = 200, no surfactant; (b) R/C = 50, no surfactant; (c) R/C = 200, CTAC/R = 0.06; (d) R/C = 200, CTAC/R = 0.1

The results from the electrical conductive testing are shown in Figure 23. Conductivity was plotted in reference to density. Density is a good indicator of porosity and weight, which are both important elements in electrodes for fuel cells. The porosity, ϵ, can be found by using Equation 5 in which $1.42\ {}^{g}/_{cm^3}$ is the pore-free density of carbon.

$$\varepsilon = \frac{1.42 - density}{1.42} \qquad \text{Eq. 5}$$

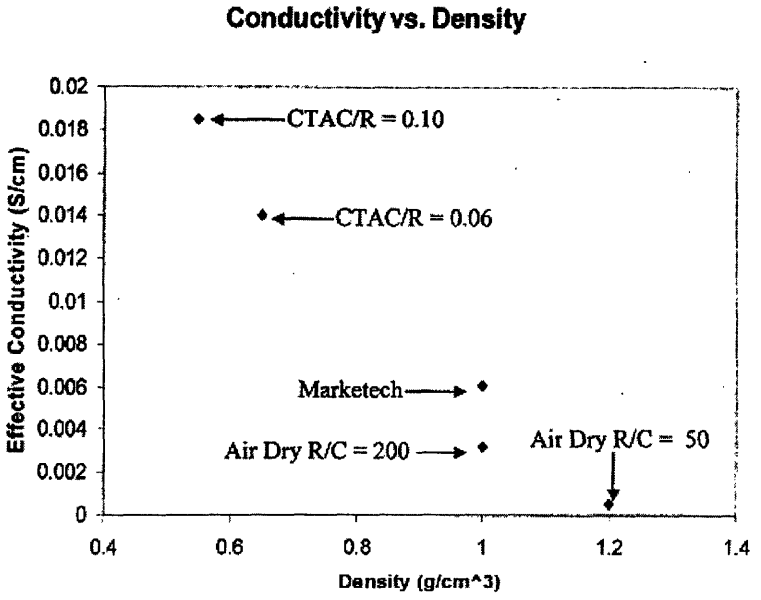

Figure 23: Effective Conductivity vs. Density for Different Carbon Aerogels. The aerogel with an R/C ratio of 200 and a CTAC/R ratio of 0.1 performed the best.

The samples in which no surfactant was used performed poorly. The aerogel with an R/C ratio of 50 and no surfactant had the lowest electrical conductivity and the highest density. The aerogel with an R/C ratio of 200 in which no surfactant was used had a slightly higher conductivity than the aerogel with an R/C ratio of 50, but still performed poorly. Both samples had a lower ionic conductivity than the standard porous carbon electrode while having a higher density.

The samples in which the R/C ratio was set at 200 and a surfactant was used demonstrated a remarkably high ionic conductivity. The sample with a CTAC/R ratio of 0.1 had an ionic conductivity that was more than three times that of the commercial electrode, at one-half the density. The sample with the CTAC/R ratio of 0.06 was denser than the sample with the higher level of surfactant and did not perform as well. However, both samples, demonstrated an ionic conductivity that was least two times that of the commercial porous carbon electrode.

Chapter 4: Carbon Aerogel Electrode Fabrication

After deciding upon carbon aerogels and researching the different aspects of fabrication, the last step was to produce a substrate which incorporated a regular and repeated design of macropores. The ability to coat the aerogel surface with a thin layer of platinum was also explored.

4.1 Die Fabrication and Filling

Initially, holes were drilled in the surface of the sample through the use of a UV laser. For preliminary work this method worked fairly well. Unfortunately, a functional electrode would need an order of magnitude more holes of a smaller diameter than the laser method could provide. Thus, it was determined that future samples would need to made through the use of a silicon die, which the gel could be poured into.

The first step was the fabrication of the silicone die. Based upon the high ratio of depth to diameter needed for the die and the small hole sizes, it was determined that the silicon die would need to made by Deep Reactive Ion Etching. Since the die was to be a negative image of the electrode, the die would need to have a series of poles corresponding to the hole locations in the electrode. The poles were designed to have a diameter of 10 micrometers with 5 micrometer spacing between poles. A mask corresponding to the pole locations was placed over a silicon wafer. DRIE was then used to remove the silicone around the poles to a depth of 100 micrometers, as seen in Figure 24.

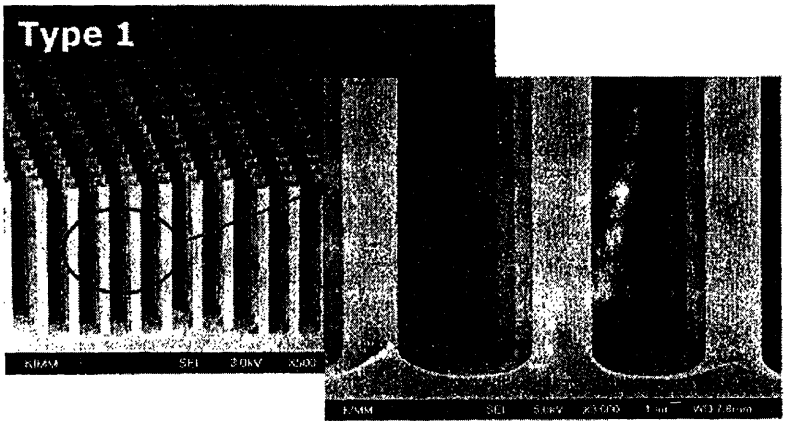

Figure 24: Image of the Silicone Die created using DRIE

After the die was fabricated, a liquid RF solution was poured over the die. The die and RF solution were then processed and allowed to dry until the solution gelled. The resulting gel was then carbonized in an inert N_2 atmosphere to create a carbon aerogel.

Several problems were discovered during initial fabrication. During DRIE, the sides of the surface features which were not be etched were coated with a thin passivating layer to protect them from the plasma used in etching. However, the protective coating was non-wetting. Since the solvent of the RF solution was water, the solution would not wet the sides of the poles. As a result, the die was not completely filled.

The solution to this problem was to treat the surface of the silicone die with O_2 plasma. The plasma eroded the protective coating from the surface of the die without significant erosion of the surface topography. As a result, the surface was much better at wetting the solution and filling of the die improved.

Another method used to improve filling was to place the samples in a vacuum chamber during the filling process. The low pressures differential caused the air within the silicone die to pass through the RF solution. The removal of the air allowed the RF solution to better fill the die and avoided air pockets which would create flaws in the final carbon aerogel electrode.

The final and most pressing problem was the cracking of the die. The high surface tension of the water within the RF solution resulted in a high level of shrinkage occurring. Due to the thinness of the poles and the high ratio of pole height to diameter, the poles could not resist the shrinkage and were bent and broken during the process. Figure 25 shows an image of a die taken after the drying process. Clear signs of the cracking and breaking of the poles can be seen. Different fabrication methods are currently being explored to correct this problem.

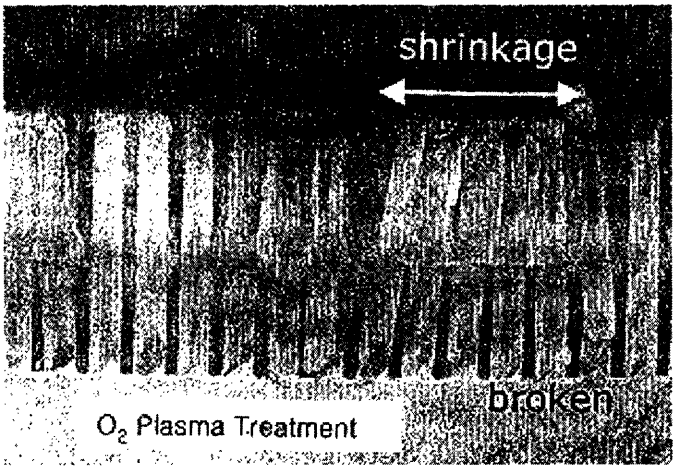

Figure 25: Image of the Breaking of the Die Caused by Aerogel Shrinkage

4.2 Platinum Coating

Thus far we have not successfully fabricated a mechanically robust dual porosity structure. For this reason, the Pt coating of the aerogel was done on a flat aerogel substrate. Electrodepositing the Pt on a substrate allowed for better imaging the Pt and made it easier to obtain its electrochemical properties.

A thin organic aerogel substrate was pyrolyzed at 1050 °C for 4 hours. During pyrolization, the sample experienced significant shrinkage and became very brittle. The brittleness

of the samples required that they be handled very carefully, and even then cracking and fractures sometimes occurred.

After pyrolization, the substrate was coated with platinum as described below. The sample was put in a holder and connected to an electrode. A non-ionic surfactant gel was then manually used to coat the sample. A 0.1 M solution of the platinum salt H_2PtCl_6 was then placed in a flask. The sample was then immersed into the solution and a -0.2 V potential was applied to the sample causing the platinum to deposit onto the surface of the sample.

Images taken of the substrate after the coating with platinum are shown in Figure 26a and 26b. The greatest contribution to the roughness of the pores was found to be from the platinum coating which had a particle height of only 100 nm. The surface of the substrate before deposition had a mirror like luster which indicated that the surface roughness was less than the wavelength of visible light. SEM images also show that the roughness of the aerogel substrate is less than 100nm. The peak height difference of the pore surface is important because during fuel cell operation it is beneficial to have the electrolyte as a smooth, even film over the pore surface. If the surface is rough, the film thickness will vary significantly and create pockets where thick electrolyte films cover the platinum deposits. Since, the oxygen atoms have to be transported through the film in order to reach the platinum catalyst, it is critical that the surface be as smooth as possible and the film of minimal thickness.

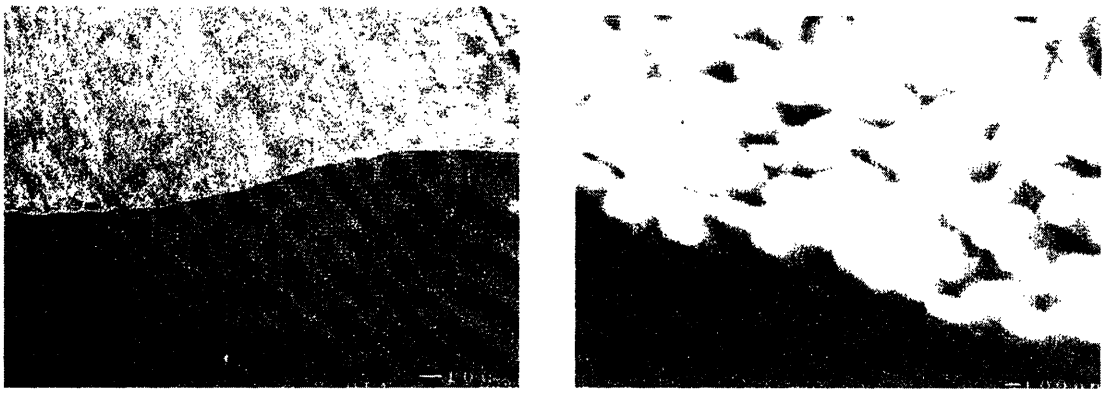

Figure 26: SEM Images of Platinum Coating of Electrode

Chapter 5: Future Improvements and Work

Significant work and progress has been made in the understanding and application of carbon aerogels for use as electrodes in fuel cells. However, several fundamental problems remain that must be solved before the technology can become commercially viable. As a result, future work needs to focus not only on optimizing the techniques used, but also on finding new and innovative solutions to these problems.

One area which will be pursued is to use alcohol as the solvent instead of water in order to solve the problem of incomplete die filling. Alcohols have the advantage of wetting almost any surface. Currently, when water based RF solutions are used to fill the die, the water does not wet to the surface of the die. Consequently, the solution has problems filling the die and the aerogel becomes flawed. The O_2 treatment mentioned earlier helps the problem but still is not a complete solution. If alcohols were uses, then the solution would wet the surface much easier and better fill the die.

The only problem is that alcohol is non-polar. As a result, current surfactants do not arrange themselves into micelle and thus cannot isolate the pores from the solvent and provide cross bracing during drying. As a result, the aerogel must be dried using super-critical CO_2, which is expensive and time consuming. Thus, work will be done to see if a surfactant can be found that allows for air drying when alcohol is used as the solvent in the same way CTAC allows for air drying of aerogels when water is used as the solvent.

Another area which needs to be pursued is how to improve the toughness of the aerogels. Currently, the carbon aerogels crack and fracture if not handled with extreme care. If this technology is to be used commercially, then the carbon aerogel electrodes will have to be tough enough to withstand the rigors of assembly and the stresses of daily operation without failing.

One of the last areas of improvement is developing a way to remove the aerogels from the die without destroying the die itself. Currently, the only way to extract the die is to place it in a chemical bath, thus dissolving the die and leaving the aerogel. However, the process of making the die is very time consuming and expensive. Since time and cost are major concerns in fuel cell fabrication, the dies must be re-usable if this technology is to be commercially viable.

Chapter 6: Conclusion

The use of carbon aerogels as the substrate for the electrodes in phosphoric acid fuel cells appears to demonstrate great potential. Testing has shown that use of a solution containing the surfactant cetyltrimethylammonium chloride (CTAC) and water can be used as the solvent in making an organic aerogel. The presence of the surfactant creates liquid crystals within the pores of the aerogel which decrease surface tension and provide structural support. As a result, the gels can be air dried rather than using super-critical CO_2 drying and still maintain the same pore structure.

Ionic Conductivity testing has demonstrated that carbon aerogels fabricated with a CTAC/R ratio of 0.1 have an ionic conductivity which is more than twice that of a commercial porous carbon substrate. Testing also showed that the replacement of the water within the pores with a substance of lower surface tension produces xerogels which have a low ionic conductivity and high density due to pore collapse.

The use of Deep Reactive Ion Etching (DRIE) has proved successful at producing a silicone die for the fabrication of an organic aerogel. However, treatment with O_2 plasma is necessary to remove the non-wetting polymer coating which remains from the DRIE process. Furthermore, even after the plasma treatment, having the RF solution wet and fill the die is still complicated and not always successful. A way to prevent die cracking and a method for removing the die from the gel are critical if the silicone dies are to be re-used.

The process of electroplating the carbon aerogel with platinum through the use a platinum salt and non-ionic gel proved very successful. The aerogel substrate is optically smooth and the deposited platinum film consists of particles with a peak height of around 100 nm. The

smoothness of the pore walls will minimize the thickness of the electrolyte film layer and thus minimize the transport time of the oxygen atoms to the platinum catalyst.

Once the remaining problems of carbon-aerogel fabrication have been solved, they can begin to be used in phosphoric acid fuel cells. The high porosity, high ionic conductivity, and short ionic and gas transport times should dramatically increase the power yield of phosphoric acid fuel cells. Hopefully, the eventual result will be the implementation of PAFCs as commercially viable medium level power sources.

References

1. Bell et. al. Mesoporous carbons and polymers. U.S. Patent 6,737,445. 18 May 2004.

2. Ritter, J.A. Effects of synthesis pH on the structure of carbon xerogels. Carbon; **1997**; Vol. 35, No. 9; pp. 1271 – 1278.

3. Pekala, R.W.; Alviso, C.T.; Kong, F.M.; Hulsey, S.S. Aerogels derived from multifunctional organic polymers. Journal of Non-Crystalline Solids; **1992**; 145; pp. 90-98.

4. Pekala, R.W.; Alviso, C.T.; LeMay, J.D. Organic aerogels: microstructural dependence of mechanical properties in compression. Journal of Non-Crystalline Solids; **1990**; 125; pp. 67-75.

5. Berthon-Fabry, Sandrine; Langohr, David; Achard, Patrick; Charrier, Daniel; Djurado, David; Ehrburger-Dolle, Françoise. Anisotropic high-surface-area carbon aerogels. Journal of Non-Crystalline Solids; **2004**; 350; pp. 136-144. http://www.sciencedirect.com/science/ article/B6TXM-4DS834R-6/2/9ac92 6f33af4397527f4661df9ce7ab8 (1 May 2005).

6. Block, V. Structural investigation of resorcinol formaldehyde and carbon aerogels using SAXS and BET. Journal of Porous Materials; 1994; 4; pp. 287 – 294.

7. Jacobson, A.M. Experimental methods in colloids and surfaces: particle surface area from gas absorption. http://www.andrew.cmu.edu/course/06607/cfe%20bet%20surface%20area.pdf (30 April 2005).

8. Zanto. Emily J. Sol-gel-derived carbon aerogels and xerogels: design of experiments approach to material synthesis. Ind. Eng. Chem Res.; 2002; 41; pp. 3151 – 3162.

9. Taylor, Hayden K. A two-level prediction model for deep reactive ion etch (DRIE). https://dspace.mit.edu/ bitstream/1721.1/7469/1/IMST031 (28 April 2005).

10. Ayón, A.A.; Lin, C.C; Braff, R.A.; Schmidt, M.A. Etching characteristics and profile control in a time multiplexed inductively coupled plasma etcher. Microsystems Technology Laboratories, Massachusetts Institute of Technology, Cambridge MA; pp 1-3.

11. Kim, Sang-Gook. Mems, Tiny Products. http://web.mit.edu/2.008/www/lectures/2.008-2005-MEMS-2.pdf (1 May 2005).